ISSN No. 231-2705 | DOI: 10.51244/IJRSI | Volume X Issue I January 2023

Computational Identification of Biomarker Signatures, Pathways and Regulators to Discover Therapeutic Target for Non-Small Cell Lung Cancer

Amina Rownaq[1*], S. M. Shahinul Islam[1], Samme Amena Tasmia[2], Md. Selim Reza[2] and Md. Nurul Haque Mollah[2]

[1]Plant Biotechnology and Genetic Engineering Lab, Institute of Biological Sciences, University of Rajshahi, Bangladesh.
[2]Bioinformatics Lab, Department of Statistics, University of Rajshahi, Bangladesh
**Correspondence Author*

Received: 28 December 2022; Accepted: 18 January 2023; Published: 06 February 2023

Abstract

Background

Lung cancer is a critical health issue of human neoplasm in worldwide. Non-small cell lung cancer (NSCLC) is the most common lung cancer from malignant disease. This study is analyses to identify biomarkers for targeting systemic drugs based on systems biology in NSCLC. The aim of this study was to select the genes expressions and pathways to discover biomolecules at protein and RNA levels which could identify potential therapeutic targets.

Methods

Different statistical method: LIMMA, ANOVA, SAM and Kruskal Wallis (KW) were used to identify DEGs with significance from the transcriptome data which was obtained from the Gene Expression Omnibus (NCBI-GEO) dataset. By using Robust Multi-Array Average (RMA) expression measure DEGs were normalized and identified from the gene expression data set and it was applied in the "Affy" package of Bioconductor platform in R. Gene expression profiles were analyzed with genome-scale biomolecular networks (i,e., protein-protein interaction, DAVID, Kaplan-Meier Plot, molecular docking).

Results

Ten (10) hub proteins and four (4) transcription factors (TFs) were significant biomarkers as a potential drug target. Risk discrimination performance of the hub proteins- AURKB, CDK1, CDC20, MAD2L1, CCNB1, BUB1, CCNB2, AURKA, NDC80 and NUF2 were also evaluated. In the molecular docking simulation study, we are suggesting Lurbinectedin, Etopophos, Entrectinib, Imatinib, mesylate, and Irinotecanas candidate drugs that have high binding affinity scores with most of the key proteins. Among 10 hub proteins two were confirmed as novel and provided a prognostic model and suggested three candidate drugs.

Conclusion

Based on these molecular signatures and proposed drugs further experimental studies can continued. These findings not only demonstrate the diagnosis, but also provide prognostic markers and therapeutic targets for NSCLC.

Keywords: Differentially expressed genes, molecular signature, molecular pathway, non-small cell lung cancer, protein-protein interaction and reporter biomolecule

I. Introduction

Lung cancer is the second major human cancer in the world. Lung cancer deaths are 1.33% of total deaths according to the latest WHO data published in May 2014 in Bangladesh. Cancer-related death rates in Bangladesh were 7.5% in 2005 and assumed it will be 13% in 2030 calculated by International Agency for Research on Cancer. Smoking is the main risk factor of lung cancer, high air pollutions and alcohol are also harmful for lung (Alberg et al., 2013). Approximately 75% of all of lung cancers are non-small cell lung cancer, which is the most common type of lung tumor in the world (Jemal et al., 2007). Based on tumor histology conventional diagnosis of lung cancer is occurred. The main histological types of NSCLC are adenocarcinoma, squamous cell carcinoma, and large cell carcinoma. Both sub-types of adenocarcinoma and squamous cell carcinoma are very dissimilar in DNA methylation, genetic mutations, transcriptome, proteome and biomarkers. Despite significant progress in the development of

ISSN No. 231-2705 | DOI: 10.51244/IJRSI | Volume X Issue I January 2023

targeted therapy, the high mortality rate in lung cancer firmly emphasizes the need for prevention and efficient detection of lung cancer, as well as a better classification, enabling patients to benefit from more specific therapy. Depend on only morphological features for lung cancer diagnoses are in many cases insufficient (D'Amico, 2008).

Gene expression profiling is used in the molecular genetic classification of cancers. Cancer is subgroups based on molecular phenotypes and the data is obtained from gene expression analyses. To decrease the high mortality rate in lung cancer is dependent on premature detection and prevents cancer risk factor while still in a curable stage. Patients are treated with surgery and/ or radiotherapy depends on the site of the primary tumor. NSCLC is often detected at an advanced stage and carries a poor prognosis. Recently, gene-expression profiling is determined by using microarrays. However, a better perception of the molecular mechanisms that discover clinical outcomes is likely to provide the basis for more effective therapeutic intervention. Questions have been raised regarding the reproducibility of microarray result and there are examples of gene expression signature that even though validated in independent patient cohorts, shows relatively little overlap of genes. It has also been stated that differential gene expression on transcript level matches protein abundance to only about 40% (Tian et al., 2004).

In this study, we have used a publicly available microarray gene expression profile dataset to identify differentially expressed genes (DEGs) by using bioinformatics methods (figure 1). The functional and pathway enrichment analysis of the DEGs was studied utilizing the gene ontology (GO). After that network analysis of DEGs with protein-protein interactions networks to identify hub proteins. We identified 10 hub proteins and 4 TFs which is associated with distant metastasis. Finally, we analyzed the molecular docking of hub genes and associated TFs, and suggested therapeutic targets with three drugs (Lurbinectedin, Etopophos, and Entrectinib) against NSCLC.

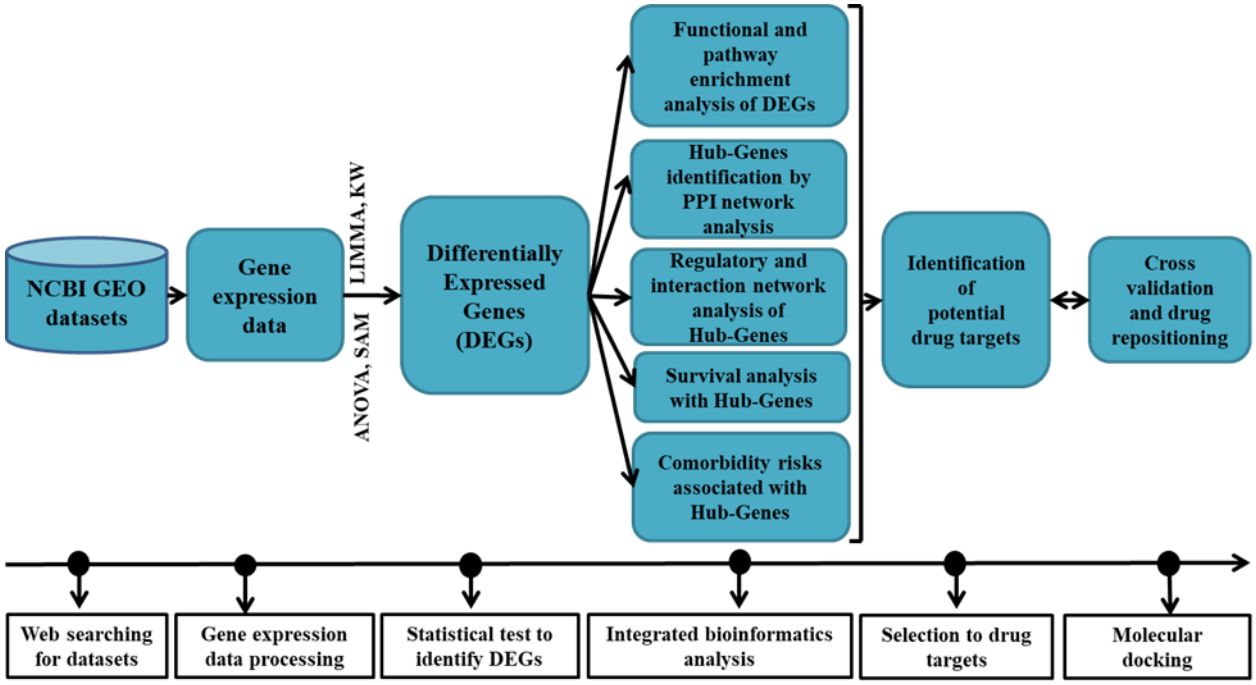

Figure 1: Pipeline of the study.

II. Materials and Methods

2.1. Gene Expression Profiling in Non-Small Cell Lung Cancer

The transcriptome data (GSE33532) for non small cell lung cancer was derived from the previous study (Michael et al., 2014) through the Gene Expression Omnibus (NCBI-GEO) dataset (Barrett et al., 2013). Gene expression profiling was hybridized from [HG-U133_Plus_2] Affymetrix Human Genome U133 Plus 2.0 Array.

2.2. Identification of Differentially Expressed Genes (DEGs)

To identify DEGs the gene expression data set was normalized through the Robust Multi-Array Average (RMA) expression measure, and it was implemented in the "Affy" package of Bioconductor platform. Different statistical method: LIMMA, ANOVA, SAM and Kruskal Wallis (KW) were used to identify DEGs with significance. The false discovery rate was controlled

ISSN No. 231-2705 | DOI: 10.51244/IJRSI | Volume X Issue I January 2023

by using multiple-testing the p-values (<0.01) which were adjusted by Benjamini Hochberg's method. All analyses packages were implemented in R (version 3.2.3), analysis was performed through the Bioconductor platform (Gentleman et al., 2004).

2.3. Gene Enrichment Analysis

By using gene overrepresentation analyses molecular function, biological process and molecular pathway annotations of the identified DEGs was find out through DAVID (Database for Annotation, Visualization and Integrated Discovery) (version v6.8) bioinformatics resources. Whole set of human genome annotation was used as the background reference set. Analyses were carried out by using Biological Process, Cellular Component, Morphological Function and Kyoto Encyclopedia of Genes and Genomes (KEGG) pathway database as the annotation sources. Statistically significant P-values (adjusted-p <0.01) were determined by using Fisher Exact test and Benjamini-Hochberg's correction.

2.4. Protein-Protein Interaction Analysis

The previously reconstructed protein-protein interaction (PPI) network of *Homo sapiens* (Karagoz et al., 2016), which consist of 288,033 physical interactions between 21,052 proteins, was recruited in the present study to construct a PPI subnetwork around the protein encoded by the identified DEGs. The sub-network was visualized and analyzed via cytoscape (v3.6.1) where nodes display the proteins and the edges display the interactions between the proteins.

To find out hub proteins a topological analysis was applied through Cyto-Hubba plugin (Chin et al., 2009) and the dual-metric approach considering degree and between's centrality metrics simultaneously were employed (Calimlioglu et al., 2015). The modules in the PPI network were identified using MCODE plug-in in Cytoscape (Chin et al., 2009).

2.5. Determination of Reporter Transcription Factors and miRNAs

Key transcriptional factor (TFs) was acquired through publicly available human transcriptional regulation interaction data bases miRNET. The reporter biomolecules feature algorithms was obtained depend on z-score and corresponding p-values of the regulatory molecules (Patil and Nielsen, 2005) (Kori et al., 2016). Statistically significant P-values (adjusted-p <0.01) were determined by using Fisher Exact test and Benjamini-Hochberg's correction.

2.6. Performance Evaluation and Cross-validation of Reporter Biomolecules

Risk assessments and survival signatures of reporter biomolecules were performed through Kaplan Meier Plotter (Gyorffy et al., 2013). According to their prognostic index and survival multivariate the patients were divided into low and high-risk group. The differences between the risk groups in gene expression levels and statistical significance of the differences was estimated through t-test and a log –rank p-value <0.01 was considered as a cut-off to describe statistical significance in all survival analyses.

2.7. Molecular docking simulation for hub gene and transcription factors

The 3-Dimension (3D) structure of 10 key proteins and 3 associated TFs were identified. Among them, the 3D structure of CDK1, CDC20, AURKB, MAD2L1, AURKA, CCNB1, BUB1, NDC80, NUF2, BRCA1, TP53, and MYC were downloaded from Protein Data Bank (PDB) (Berman et al., 2002) with the PBD codes 4y72, 4ggc, 4af3, 1go4, 1muo, 2jgz, 4a1g, 2igp, 2ve7, 1mdi, 1a1u, and 1a93 and CCNB2 target was downloaded from SWISS-MODEL using UniProt (Waterhouse et al., 2018); The Uniport onsortiam) with IDO95067 respectively. The 3D structures of 110 FDA-approved drugs were downloaded from PubChem database (Kim et al., 2019) seen in the supplementary Table-S1. Interactions of the key proteins and associated TFs with candidate's drugs were calculated based on their binding affinities (kcal/mol). The 3D structure of targets was visualized using Discovery Studio Visualizer 2019 and the water molecules, co-crystal ligands which were bound to the protein were removed. Further, the protein was prepared using USCF Chimera and Autodock vina in PyRx open-source software by adding charges and minimizing the energy of the protein, and subsequently converting it to pdbqt format (Pettersen et al., 2004; Trott et al., 2010; Dallakyan et al., 2015). The exhaustiveness parameter was set to 8. The Protein-Ligand Interaction Profiler (PLIP) web service (Salentin et al., 2015) and PyMol (DeLano et al., 2002) was used to analyze the docked complexes for surface complexes, types and distances of non-covalent bonds.

2.8. Gene Disease Interaction

The association of ten hub genes CDK1, CDC20, AURKB, MAD2L1, AURKA, CCNB1, BUB1, NDC80, NUF2 and CCNB2 with human disease is discover from publicly available DisGeNET (Janet et al., 2020) datasets. CURATED databases are considerd as a source for this experiment which are from UniProt, PsyGeNET, Orphanet, the CGI, CTD (human data), ClinGen, and the Genomics England PanelApp.

ISSN No. 231-2705 | DOI: 10.51244/IJRSI | Volume X Issue I January 2023

2.9. Analysis Methods

i. Analysis of Variance (ANOVA)

Analysis of variance is a parametric test. In experimental design and data analysis, the Analysis of Variance (ANOVA) is one of the most widely used basic statistical techniques. This is most used for the discovery of DE genes between two or more conditions. ANOVA is used to compare the mean of several populations. The null and alternative hypotheses are:

H_0:$\mu_1 = \mu_2 = \ldots\ldots = \mu_k$

H_1 : $H_0$is false ("at least one population mean differs")

Where, μi represents the population mean of group i.

Test Statistic:

$$Fi = \frac{Between\ group\ variance}{Wit\square in\ group\ variance} = \frac{\frac{SSBetween}{(m-1)}}{\frac{SSWit\square in}{(n-m)}} = \frac{MSBetween}{MSWit\square in}$$

Where, MS and SS denote the mean sum of square and sum of square respectively and also $n=n_1+n_2+,\ldots,n_K$The Fi follows the *F*-distribution with (m-1) and(n-*m*) degrees of freedom under H0. Note that this *F* statistic follows *t*-statistic with (*n*1+*n*2-2) degrees of freedom for k=2.

ii. Kruskal Wallis (KW)

The Kruskal Wallis test is the non-parametric alternative to the One Way ANOVA. Non parametric means that the test doesn't assume the data comes from a particular distribution. The kw test is an extension of the Wilcoxon test and can be used to test the hypothesis that several unpaired samples originate from the same population. The hypotheses for the test are:

H_0: $m_1 = m_2 = \ldots\ldots = m_k$

H_1: H_0 is false ("at least one population median differs").

Where, m_i represents the population median of group i.

Test statistic: s^2

$$T = \frac{1}{s2}\left[\sum_{k=1}^{m} \quad \frac{Rk}{nk} - n\frac{(n+1)2}{4}\right]$$

Where n is the total number of samples and Rk is the sum of the ranks for k^{th}group and,

$$s2 = \frac{1}{n-1}\sum_{i,k} \quad Rik2 - n\frac{(n+1)2}{4}]$$

The null hypothesis of the test is that all *m* distribution functions are equal and the alternative hypothesis is that at least one of the populations differs from the others.

iii. Significance Analysis of Microarrays (SAM)

Significance analysis of microarrays (SAM) is a statistical technique is established (Tusher et al., 2001) for determining whether changes in gene expression are statistically significant. It controls the false discovery rate (FDR) by sharing information of all genes. It does not suffer from the small- sample sizes and normality assumptions.

Test Statistic:

$t_i^{SAM} = \frac{ri}{si+s0}$

where, $r_i = \underline{yi1} - \underline{yi2}$ and s_i are the pooled variances and $s_0$has been computed as the 90th percentile of the standard error of all genes.

ISSN No. 231-2705 | DOI: 10.51244/IJRSI | Volume X Issue I January 2023

iv. The Linear Models for Microarray (LIMMA)

The linear models for microarray (LIMMA) were developed by (Smyth et al., 2003) It is also the moderated version of *t*-statistic. The test statistic for LIMMA is defined by:

$$t_i^{LIMMA} = \frac{r_i}{s_i^{LImma}\sqrt{(\frac{1}{n_1}+\frac{1}{n_2})}}$$

It has the same interpretation like *t*-test except that the standard errors have been moderated across the genes. In this test, the posterior variances, s_i^{LImma} have been substituted in the place of usual variances of the *t*-test.

v. Robust Multi-array Average (RMA) expression measure

Robust Multi-array Average (RMA) expression measure is proposed by (Irizarry et al., 2003). The expression of a target gene is represented by the calculated signal intensity of a probeset on an Affymetrix GeneChip. The RMA model is defined by:

$$y_{kij}=m_k+\square_{ki}+\square_{kj}+\square_{kij}$$

Where, $\square_{ki}$ is a prob-effect ; i=1…I , $\square_{kj}$ is chip-effect ($m_k + \beta_{kj}$ is log2 gene expression on array j) ; j=1…J, k=1…K, is the number of probsets.

vi. False Discovery Rate (FDR)

The false discovery rate (FDR) is the expected proportion of type I errors. A type I error is where you incorrectly reject the null hypothesis. The formula of FDR is defined by: FDR = E(V/R | R > 0) P(R > 0)

Where, V is the number of Type I errors (i.e. false positives) and R is number of rejected hypotheses.

Benjamini-Hochberg's Method:

The Benjamini-Hochberg Procedure is a powerful tool that decreases the false discovery rate. The formula is defined by:

$$BH= (i/m)Q$$

Where, i is the individual p-value's rank, m is the total number of tests, and Q is the false discovery rate (a percentage).

III. Results

3.1. Genome Reprogramming in Non-Small Cell Lung Cancer

In this study, four statistical methods were used to identify DEGs from noise and outliers in the transcriptome dataset. The parametric method LIMMA, ANOVA, SAM and Kruskal Wallis (KW) was used to identify DEGs with statistical significance of adjusted p<0.01. Separately, LIMMA identified 533 DEGs, ANOVA identified 543 DEGs, SAM identified 535 DEGs and KW identified 556 DEGs. Among those four statistical tests 291 differential expressed genes were common (figure 2), whereas 105 genes were up regulated and 186 genes down regulated. These DEGs were considered in further analysis.

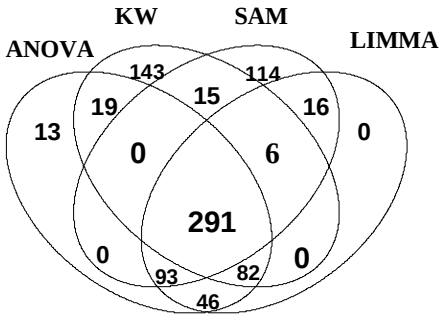

Figure 2: Identification of DEGs in non small cell lung cancer by using different parametric methods.

ISSN No. 231-2705 | DOI: 10.51244/IJRSI | Volume X Issue I January 2023

GO categories and KEGG pathways were identified by uploading all DEGs to DAVID. To formulate the molecular functions, biological processes, cellular components and KEGG pathways functional overrepresentation were associated with proteins encoded by the DEGs. GO analysis was performed by DAVID results which represent that up regulated DEGs are significantly enriched in biological processes (BP), cellular component (CC) and molecular function (MF) and down regulated DEGs are less significant for this study (Table 1).

The up regulated DEGs and down regulated DEGs both are analyzed in KEGG pathway analysis. The results are represented up regulation and down regulation of pathways in Progesterone-mediated oocyte maturation, p53 signaling pathway, Oocyte meiosis and cell cycle (Figure 3).

Table 1: Gene enrichment analysis of differentially expressed genes in non small cell lung cancer and hub genes are mentioned as bold.

Up Regulated Gene				
Category	Gene Function/ Terms	No. of gene	P-Value	Gene Name
BP	mitotic nuclear division	10	3.7E-6	**BUB1, NDC80, NUF2, AURKA, AURKB, CCNB2, CDK1**, KLHL42, PLK5, SMC5
	cell division	11	8.6E-6	**BUB1, MAD2L1, NDC80, NUF2, AURKA, CCNB1, CCNB2, CDK1,** KLHL42, PLK5, SMC5
	sister chromatid cohesion	6	1.6E-4	**BUB1, MAD2L1, NDC80, NUF2, AURKB,** SMC5
	protein autophosphorylation	6	1.6E-3	EPHA8, **AURKA, AURKB**, CAMK2B, PAK1,TKN1
CC	kinetochore	5	7.5E-4	APC**, BUB1, MAD2L1,NDC8O, AURKB**
	condensed chromosome kinetochore	4	9.7E-3	**BUB1, MAD2L1,NDC8O, NUF2**
MF	protein kinase activity	8	1.8E-3	**BUB1, AURKA, AURKB,** CAMK2B, **CDK1**, PAK1, PLK5, TTBK1
	protein serine/threonine kinase activity	7	9.9E-3	**BUB1, AURKA, AURKB,** CAMK2B, **CDK1**, PAK1, TTBK1
Down Regulated Gene				

ISSN No. 231-2705 | DOI: 10.51244/IJRSI | Volume X Issue I January 2023

Category	Gene Function/ Terms	No. Of gene	P-Value	Gene Name
BP	protein phosphorylation	7	6.2E-2	CDC42BPB, HIPK2, MAP3K8, PIK3CD, PRKCH, ZAK,TNK1
	small GTPase mediated signal transduction	5	6.5E-2	DNAJC27, ARHGAP31, CHP1, RHOJ, RHOQ
	negative regulation of transcription, DNA-templated	9	1.2E-2	KLF11, LRRFIP1, RUNX1T1, TBX3, ATXN1, PRMT2, Tceal7, ZEB1, ZHX3
CC	cell-cell adherens junction	4	3.5E-1	LRRFIP1, PPFIBP1, FMNL2, RTN4
MF	ATP binding	15	7.5E-2	CDC42BPB, DHX38, ACTG2, ACSS3, BMPR2, CHD9, DICER1, HIPK2, MAP3K8, MYH10, PIK3CD, PRKCH, ZAK, TTBK2, TNK1
	protein serine/threonine kinase activity	6	8.3E-2	CDC42BPB, HIPK2, MAP3K8, PRKCH, ZAK, TTBK2

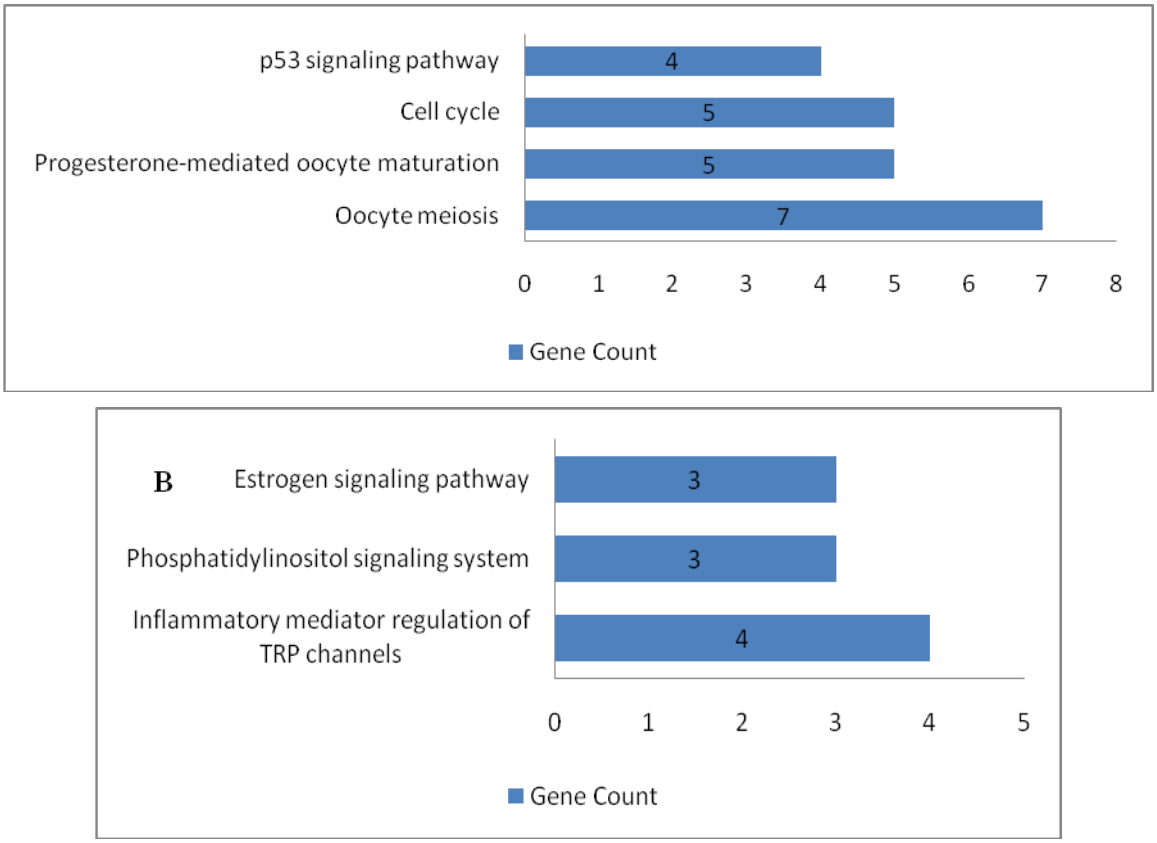

Figure 3: KEGG pathways were identified based on the DEGs. A. KEGG pathways of up-regulatory DEGs and B. KEGG pathways of down-regulatory DEGs.

ISSN No. 231-2705 | DOI: 10.51244/IJRSI | Volume X Issue I January 2023

3.2. Proteomic Signatures in Non-Small Cell Lung Cancer

Hub proteins have a significant role in signal transduction events during disease progression. Hub proteins were identified through a PPI sub-network which was constructed around proteins encoded by the DEGs via their physical interactions and topological analysis. As a result, ten hub proteins were found (Figure 4 and Table 2) and those are AURKB, CDK1, CDC20, MAD2L1, CCNB1, BUB1, CCNB2, AURKA, NDC80 and NUF2.

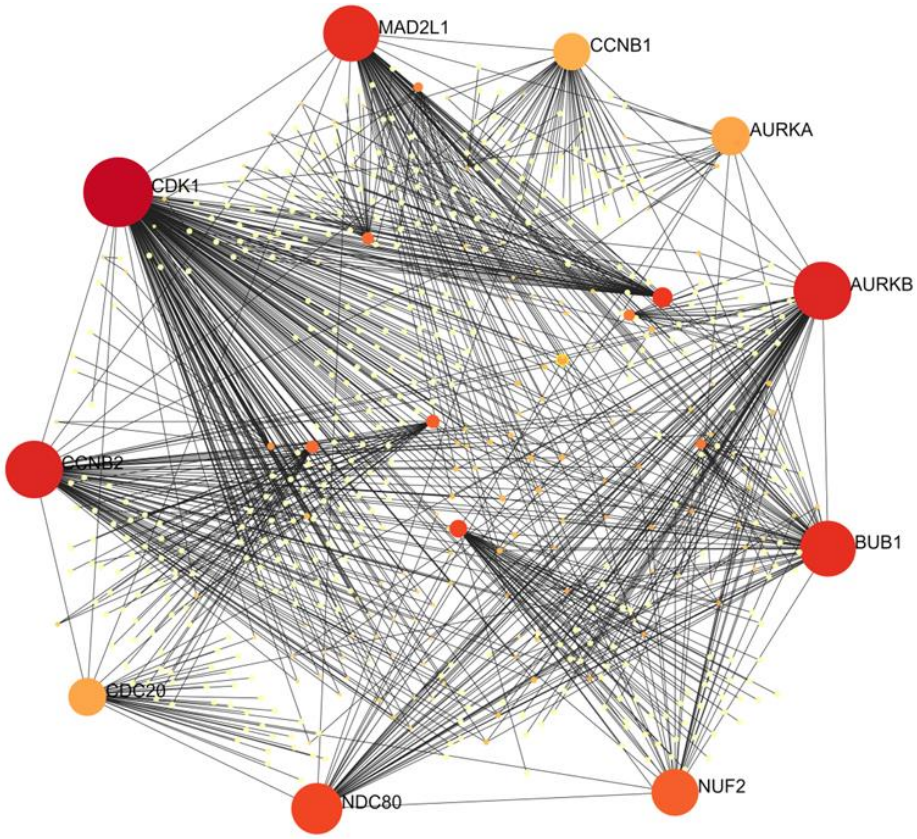

Figure 4: Hub proteins were obtained from protein-protein interaction networks of the DEGs in non small cell lung cancer. Here, red to yellow colors represent the hub proteins. The nodes indicate the DEGs and the edges indicate the interactions between two genes.

Table 2: Statistically significant value of hub proteins in non small cell lung cancer and some references which support that these hub genes are responsible for cancer.

Hub Proteins	Adj.P.val	Hazard ratio(TCGA)	References
AURKB (This gene encodes a member of the aurora kinase subfamily of serine/threonine kinases)	8.20E-13	1.84	Wang et al., (2020), Huang et al., (2019),
CDK1 (Cyclin-dependent kinase 1)	3.28E-16	NA	Nie et al., (2020), Xie et al., (2019)
CDC20 (Cell division cycle protein 20 homolog)	5.30E-01	1.82	Cheng et al., (2019), Zhuang et al., (2018)

ISSN No. 231-2705 | DOI: 10.51244/IJRSI | Volume X Issue I January 2023

MAD2L1 (Mitotic Arrest Deficient 2 Like 1)	1.69E-17	1.55	Liu et al., (2019), Pabla et al., (2019)
CCNB1 (Cyclin B1)	6.82E-01	1.63	Wang et al., (2020), Xiao et al., (2018)
BUB1 (mitotic checkpoint serine/threonine kinase)	3.89E-13	1.83	Tang et al., (2019), Ocaña et al., (2016)
CCNB2 (Cyclin B2)	1.98E-18	1.99	Qin et al., (2020), Xu et al., (2018)
AURKA (Aurora Kinase A)	1.53E-10	1.52	Gautam et al., (2019) Komoto et al., (2018)
NDC80 (Component of the NDC80 complex)	1.85E-14	1.47	Zhong-Yi et al., (2020), Elena (2010)
NUF2 (Kinetochore protein Nuf2)	2.60E-13	2.02	Li et al., (2022), Peng et al., (2015)

3.3. Key TFs from TFs-HGs Network

Key Transcriptional factors are obtained from TFs and hub genes (HGs) interaction network, where red color cycle indicates the genes and green color circle indicates the TFs and larger size indicates higher degree (figure 5). Total four TFs such as TP53, MYC, BRCA1 and EP300 were found as key TFs.

3.4. Key miRNAs from miRNAs-HGs Network

miRNAs (microRNAs)-hub genes interaction network is represented in figure 5, where red color cycle indicates the genes and blue color indicates the miRNAs and larger size indicates higher degree. Top degree miRNAs were selected from miRNAs-hub protein interaction network with degree > 7 and degree >= 2 respectively. Common miRNAs were extracted and considered those as key miRNAs. Total three key miRNAs such as hsa-mir-16-5p, hsa-mir-34a-5p and has-mir-1-3p were found.

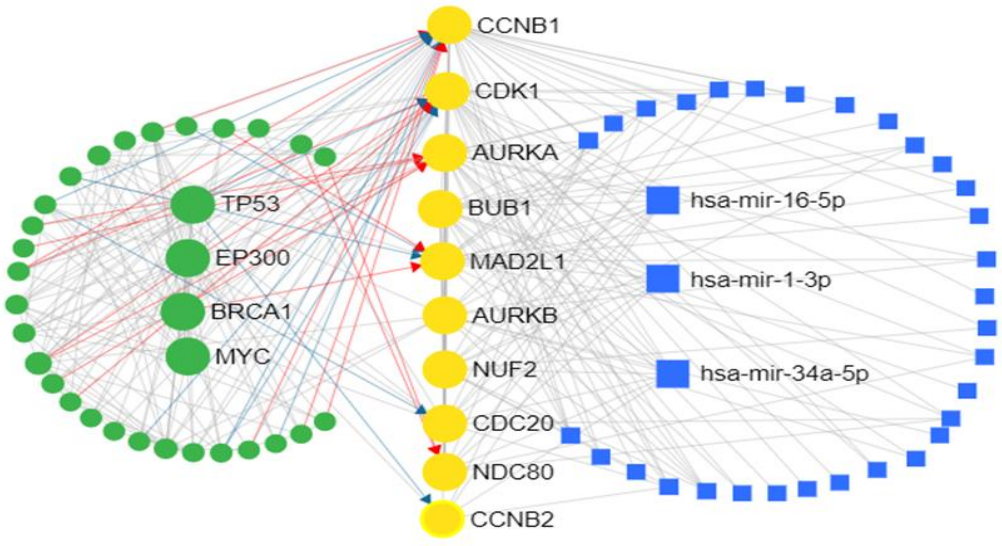

Figure 5: Interaction network of HGs-TFs (A), HGs-miRNA (B) and HGs-TFs-miRNA (C). Where red cycle indicates the genes, green cycle indicates the TFs and blue color indicates the miRNAs (A-C) and larger size indicates higher degree.

ISSN No. 231-2705 | DOI: 10.51244/IJRSI | Volume X Issue I January 2023

3.5. Analysis of Cross-validation and Risk Discrimination Performance

The differential expression signatures were authenticated and the analysis of the risk discrimination performance of 10 hub proteins was performed by using independent RNA-seq dataset which is acquire from TCGA. Considering their risk discrimination performance, the samples were divided into two groups and these groups are entitled as low-risk and high-risk. The gene expression differences in the levels between the two risk groups were presented based on survival data which were analyzed in Kaplan-Meier plots. Following the hub gene upload, 9 genes were available in kmplot database and CDK1 gene was unavailable. Among these 9 genes, 7 of which were a significantly associated with low survival rates whereas, NDC80 and AURKA has less significant association (P<0.01; figure 6).

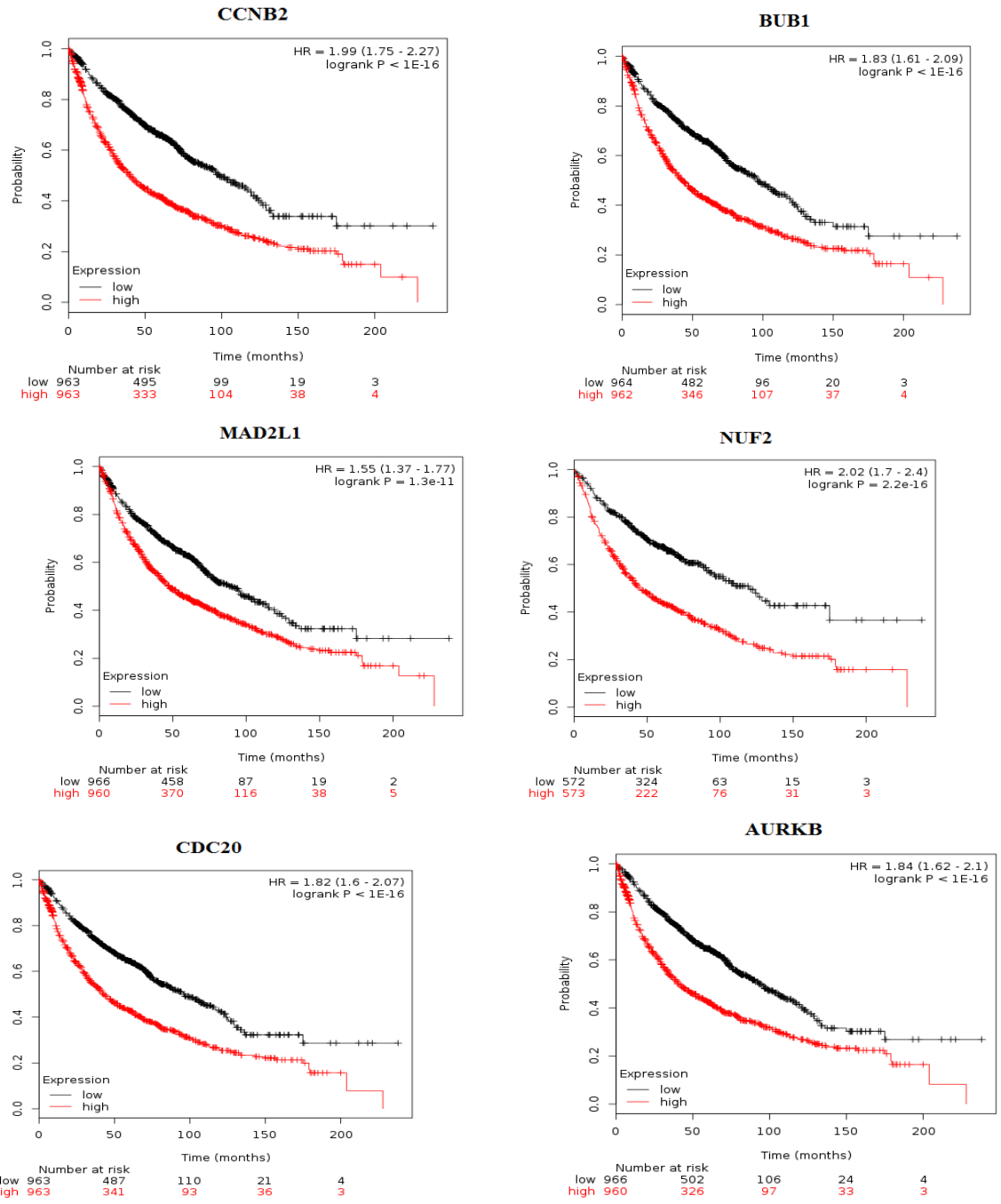

ISSN No. 231-2705 | DOI: 10.51244/IJRSI | Volume X Issue I January 2023

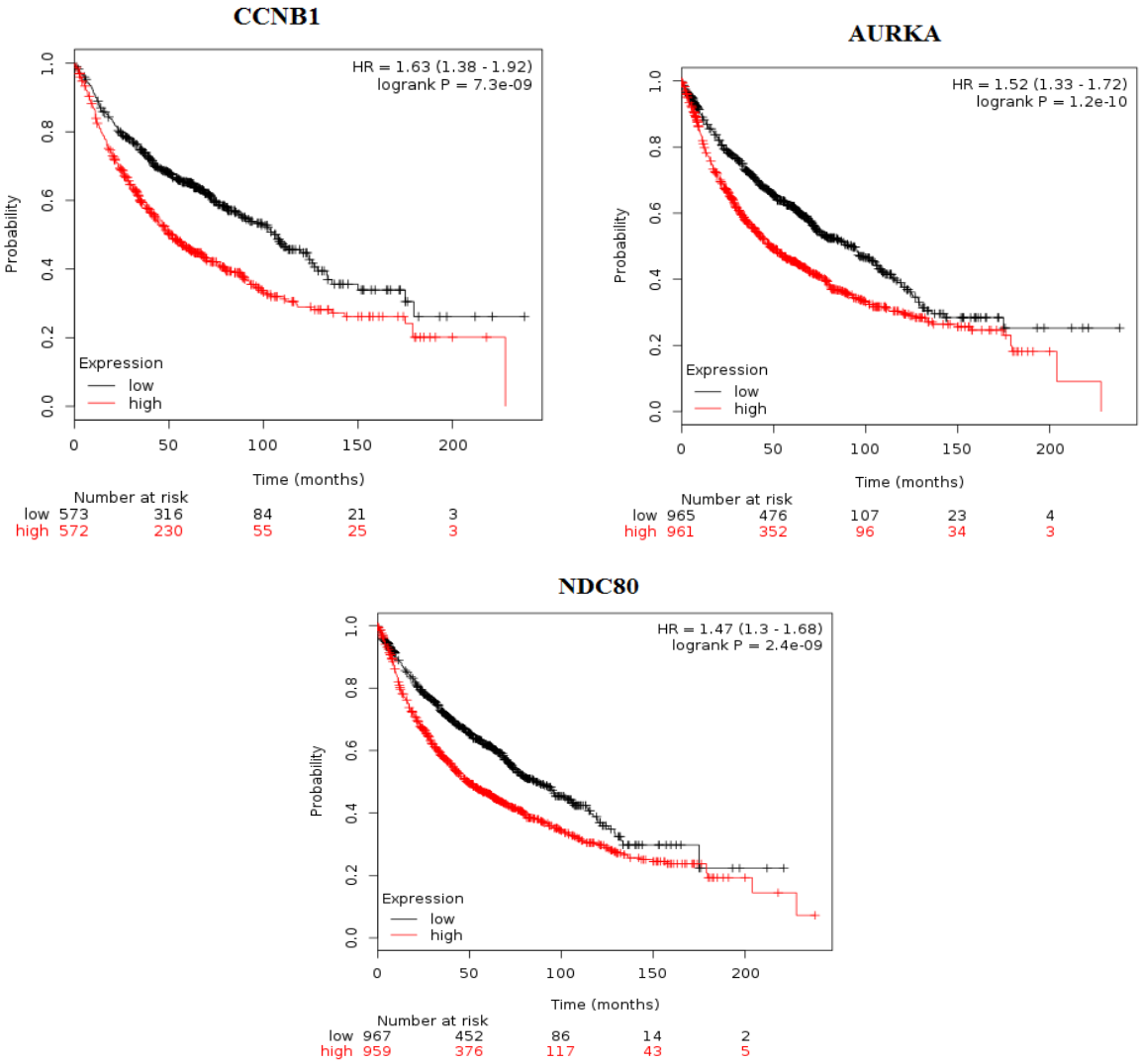

Figure 6: Cross validation and prognostic performance analyses of hub proteins. Kaplan-Meier plots are representing the prognostic power of all hub proteins in NSCLC. CCNB2, BUB1, MAD2L1, NUF2, CDC20, AURKB and CCNB1 are significantly associated with low survival rate and AURKA and NDC80 has less significant association ($p<0.01$).

3.6. Drug Repositioning by Molecular Docking Analysis

Molecular docking simulations were performed to identify candidate drugs for the key proteins and associated TFs. The result of binding affinities is given in (figure 7). The list of compounds whose binding affinities score lies between (-9.9 to -9.9) kcal/mol with key proteins and associated TFs in Table T1. As a result, highest binding affinities lies between (-9.9 to -9.5) kcal/mol of protein CDK1 with 19 lead compounds which are Lurbinectedin, Etopophos, Entrectinib, Larotrectinib, Dacomitinib, Alpelisib, Imatinibmesylate, Abemaciclib, Abiraterone, Duvelisib, Lenvatinib, Daunorubicin, Epirubicin, Copanlisib, Afatinib, Dabrafenib, Histrelin, and Erdafitinib. The protein CDC20 with 13 lead compounds which are Lurbinectedin, Etopophos, Entrectinib, Lapatinib, Apalutamide, Duvelisib, Enasidenib, Eribulin, Imatinibmesylate, Dabrafenib, Etoposide, and Fosaprepitantwith highest binding affinities lies between (-9.9 to -9.5) kcal/mol. The protein AURKA with 6 lead compounds which are Lurbinectedin, Avapritinib, Etopophos, Etoposide, Entrectinib, and Imatinibmesylate. The proteinMAD2L1 with6 lead compounds which are Lurbinectedin, Ibrutinib, Abiraterone, Dabrafenib, Daunorubicin, and Dacomitinib. The protein AURKB with 6 lead compounds which are Lapatinib, Darolutamide, Lurbinectedin, Entrectinib, Alpelisib, and Cabozantinib.The protein CCNB2 and BUB1 lead only with compound Abemaciclib and Lurbinectedin respectively.

ISSN No. 231-2705 | DOI: 10.51244/IJRSI | Volume X Issue I January 2023

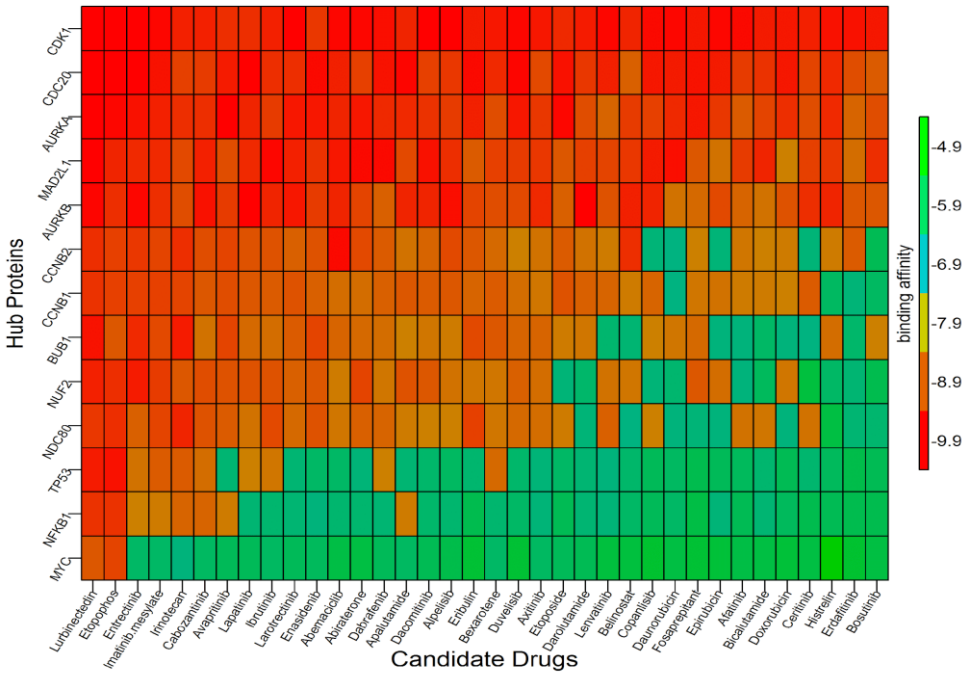

Figure 7: Drug repositioning of identified hub genes and associated transcription factors by using molecular docking simulation.

Although the rest of the proteins did not bind to any of the compounds lies between (-9.9 to -9.5) kcal/mol of binding affinity score but the overall result is good. As a result, four small chemicals Lurbinectedin, Etopophos, Entrectinib, Imatinibmesylate bind with most of the targets showing better binding affinity score. Finally, it was proposed that Lurbinectedin, Etopophos, Entrectinib might be candidate drugs for the non small cell lung cancer treatment (Table 3).

Table 3: Top 2 potential targets and top 3 lead compounds based on docking results. Lead three compounds Lurbinectedin, Etopophos, and Entrectinibwere selected by investigating the binding affinity score. The 2D structures of lead compounds are shown in 2nd column. The 3D structure of hub protein with candidate drugs is shown in 4th column. The 2D Schematic diagram of hub protein with candidate drugs interaction is given 5th column and neighbor residues (within 4 Å of the drug) are shown. Key interactions amino acids and their binding with potential targets were shown in the last column.

Potential Targets	Structure of Lead Compounds	Binding Affinity # (kCal/ mol)	The 3d view of complex	Ligand Interactions	Interacting Amino Acids			
					Hydrogen bond	Hydrophobic Interactions	Halogen/ Salt Bridge	π-Stacking/π-Cation
CDK1	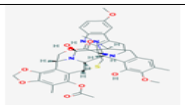 Lurbinectedin	-9.9	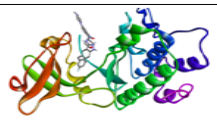	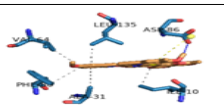	Asp86	Ile10, Ala31, Val64, Phe80, Leu135	Asp86	-
CDC20	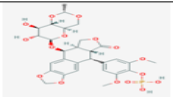 Etopophos	-9.9		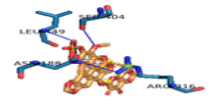	Asn188, Arg316,Ser404, Leu449	Asn188	Arg316	Arg316
CDK1	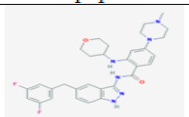 Entrectinib	-9.9	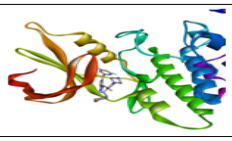	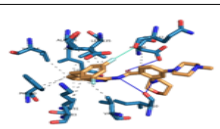	Ile10, Eu83, Asp86	Val18, Ala31, Lys33, Val64, Phe80, Asp86, Leu135, Ala145, Asp146	Gln132	-

ISSN No. 231-2705 | DOI: 10.51244/IJRSI | Volume X Issue I January 2023

3.7. Gene Disease Interaction

Genes are responsible for different diseases. Ten hub genes association with human disease are discover from publicly available DisGeNET datasets. The gene-disease information in DisGeNET is occurred from different type of databases. CURATED databases are considerd as a source for this experiment which are from UniProt, PsyGeNET, Orphanet, the CGI, CTD (human data), ClinGen, and the Genomics England PanelApp (Figure 8). Among these ten hub genes nine genes (except CCNB1) are responsible for Liver carcinoma. We have proposed three candidate drugs Lurbinectedin, Etopophos, Entrectinib for NSCLC, which also could propose for liver carcinoma.

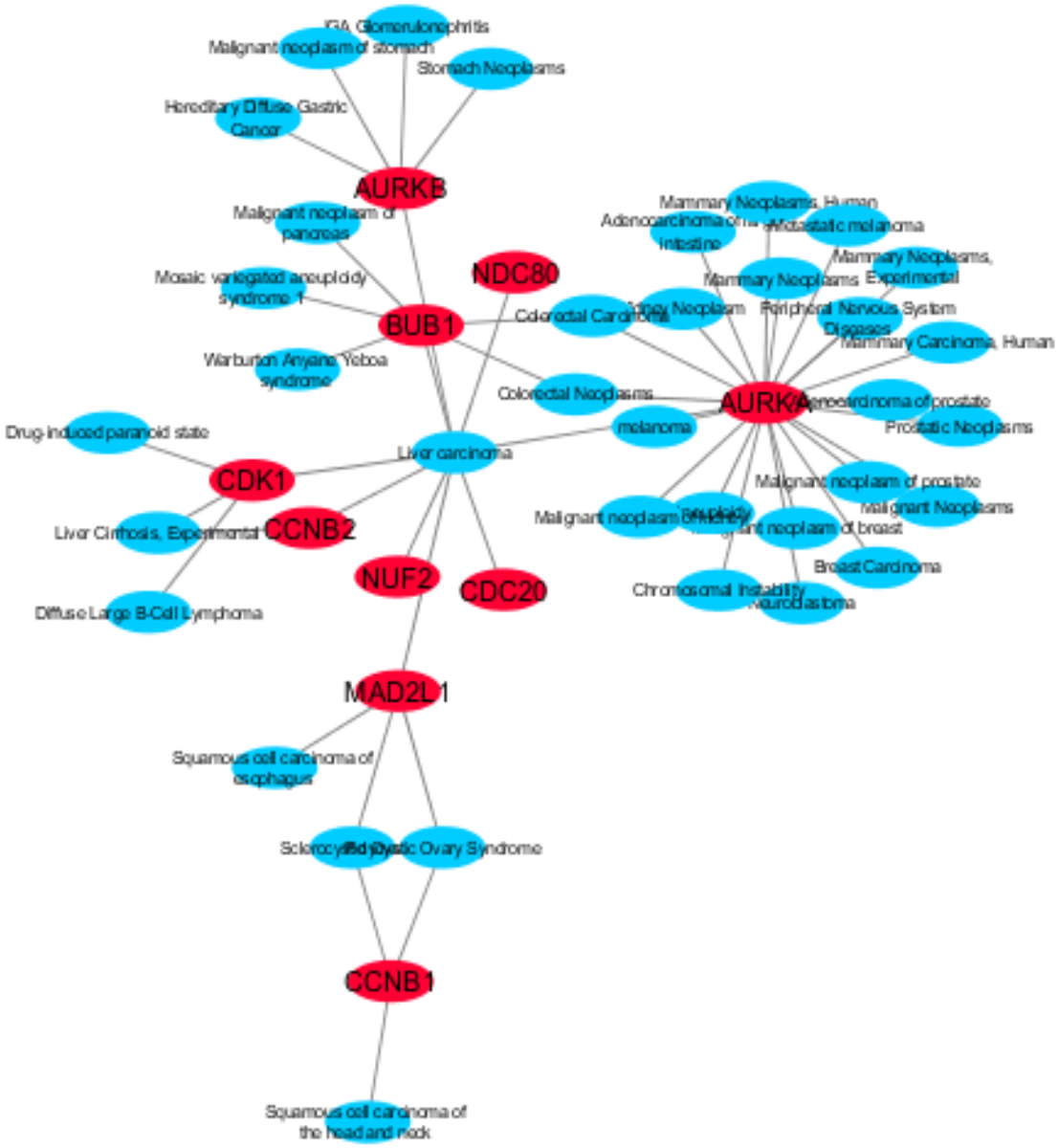

Figure 8: Gene-disease interaction network of hub genes, where red color indicates genes and blue color indicates disease.

IV. Discussion

The frequency and fatality of NSCLC are high among the neoplasm diseases worldwide and the disease has been studied comprehensively, there is still a need for more precise diagnostic and prognostic markers for the disease's development. In this study, we followed a multi-omics data combination framework to expose molecular signatures at mRNA and protein levels,

ISSN No. 231-2705 | DOI: 10.51244/IJRSI | Volume X Issue I January 2023

which offers the promise as biomarkers and potential drug targets for efficient treatments. We performed several analyses of NSCLC, including GO, identify new biomarker, a comparison of gene expression profiles, analysis of patient survival rate and molecular docking.

The Differential Expression Genes (DEGs) were found total of 291 DEGs by analysis of gene expression profiles in lung cancer samples with statistically significant changes in their expression profiles. Current studies demonstrate the significance of tumor microenvironment as a crucial factor in tumorigenesis in various cancers (Dzobo et al., 2016, Gollapalli et al., 2017, Gov et al., 2017, Hu et al., 2017, Miskolczi et al., 2018). GO analysis of statistically significant for both up and down DEGs in NSCLC to uncovered biological processes, cellular component and molecular function (Table 1).

To solve different ascending problem associated with diseases such as identifying effective biomarkers and therapeutic targets for correct diagnosis, prognosis, and therapeutics, the reconstruction of accurate PPI sub-networks is important (Sevimoglu and Arga, 2014, Turanli and Arga, 2017). We identified hub protein by reconstructing a PPI sub-network around the DEGs in NSCLC based on the topology which have the significant contribution to the progression of cancers (Table 2).

We have evaluated the binding affinity of the 108 FDA-approved drugs with the identified Key targets and associated TFs. As a result, we have got ten drugs (Lurbinectedin, Etopophos, Entrectinib, Imatinibmesylate, Irinotecan, Cabozantinib, Avapritinib, Lapatinib, Ibrutinib, Larotrectinib) that binding with five targets (CDK1, CDC20, AURKA, MAD2L1, and AURKB). Finally, we have suggested the three leading compounds lurbinectedin, etopophos, and entrectinib against potential targets CDK1 and CDC20 respectively due to maximum binding affinities with score -9.9 kCal/mol. And others important potential targets and small compounds are show in supplementary Table-S3.

On the other hand, lurbinectedin (ZEPZELCA) was an effective treatment for PS (platinum-sensitive) relapsedsmall-cell lung cancer (SCLC), especially in patients with chemotherapy-free interval (CTFI)≥180 days, with acceptable safety and tolerability (VivekSubbiah et al., 2020). Besides, Lurbinectedin was a selective inhibitor of oncogenic transcription that binds preferentially to guanines located in the GC-rich regulatory areas of DNA gene promoters (Leal et al., 2010; Nunez et al., 2016). Lurbinectedinalsoaffects the tumor microenvironment landscape by inhibiting activated transcription in tumor-associated macrophages (Belgiovine et al., 2017). Recently, in June 2020, the team from US FDA granted accelerated approval to lurbinectedin for adult patients with metastatic SCLC with disease progression on or after platinum-based chemotherapy based on results from a phase II study (study B-005; NCT02454972). This key study showed amazing antitumor activity in 60 SCLC patients with CTFI $\geq$ 90 days treated with lurbinectedin as second-line: ORR of 45.0 %, median duration of response of 6.2 months and median OS of 11.9 months (Trigo et al., 2020). The combined therapy of etopophos (VP-16) and carboplatin (DDP) had the capable to inhibition of autophagy by induced overexpression of miR-24-3p helps resensitize SCLC cells with concentration of 1.5μg/ml VP16 and concentration of 1.25μg/ml DDP (Pan et al., 2015). Also, the amalgamation of VP16–DDP is the broadly used systemic therapy for SCLC, especially for advanced-stage disease (Kuo et al., 2012). Moreover, etopophoswith carboplatin have been selected as standard treatment for SCLC since long back (Kurup et al., 2004; Nowak et al., 2006). Entrectinibhad the capability to inhibit purified ALK, ROS1 and NTRK in different tumor types harboring rearrangements in these genes, among of them ROS1--positive NSCLC (Facchinetti et al., 2019). Of interest, in August 2019 FDA has been granted entrectiniban accelerated approval for the treatment of ROS1-rearranged NSCLC, as well as of NTRK fusion–positive solid tumors (FDA, 2019). Though experiments on human positivetumor cells were performed in TRK- and ALK-driven models only, the activity of entrectinib was tested on engineered ROS1-dependent Ba/F3 cells models, in which the drug confirmed an IC50 of 5 nM (Menichincheriet al., 2016; Ardini et al., 2016).

So our findings are 13 key genes with two novel genes, which may target therapy for NSCLC. Moreover, lurbinectedin, etopophos, and entrectinibwould be the best candidate drugs that were docked effectively to targets (Table 3). In the light of the findings, CDK1 and CDC20 were the preeminent hub proteins when we consider the molecular docking results with all repurposed candidate drugs.

V. Conclusion

In this study, transcriptome data were combined with genome-scale biological networks to expose molecular signatures at RNA and protein levels. We identified 10 hub proteins (AURKB, CDK1, CDC20, MAD2L1, CCNB1, BUB1, CCNB2, AURKA, NDC80 and NUF2) and 4 TFs (TP53, MYC, BRCA1 and EP300) among them 2 are novel (CDK1 and CDC20) and showed the effect of the expression level on NSCLC patient survival. The differential expression profiles of biomolecules were cross validated in independent RNA-seq datasets. By using the molecular docking simulation study, three lead compounds of lurbinectedin, etopophos, and entrectinib were selected as the prominent drug candidate molecules since their higher binding affinity score with the reported key proteins and associated TFs. The result of this study will not only contribute to clarifying the diagnosis but also provide prognostic markers and therapeutic targets for NSCLC.

ISSN No. 231-2705 | DOI: 10.51244/IJRSI | Volume X Issue I January 2023

Competing interests

There is no conflict of interest exists. We hope to confirm that there are no any known conflicts of interest which are associated with this publication.

Acknowledgements

We are grateful to Institute of Biological Sciences, University of Rajshahi, Rajshahi, Bangladesh and Lab of Bioinformatics, Department of Statistics, University of Rajshahi, Rajshahi, Bangladesh for providing this research facility.

Funding

Fund (NST scholarship) achieved from Ministry of Science and Technology (MOST), Bangladesh. This research also funded by Institute of Biological Sciences, University of Rajshahi, Bangladesh.

References

1. Alberg AJ, Brock MV, Ford JG, Samet JM and Spivack SD (2013). Epidemiology of lung cancer: Diagnosis and management of lung cancer. Third Edition: American College of Chest Physicians evidence-based clinical practice guidelines. Chest 143: e1S, e29S.
2. Ardini E, Menichincheri M, Banfi P, (2016) Entrectinib, a pan-TRK, ROS1, and ALK inhibitor with activity in multiple molecularly defined cancer indications. Mol Cancer Ther.;15(4):628–639. doi:10.1158/1535-7163.MCT-15-0758.
3. Barrett T, Wilhite SE, Ledoux P, Evangelista C, Kim IF, Tomashevsky M, Marshall 1 KA, Phillippy KH, Sherman PM, Holko M, Yefanov A, Lee H, Zhang N, Robertson CL, Serova N, Davis S, Alexandra Soboleva A (2013). NCBI GEO: Archive for functional genomics data sets - Update. Nucleic Acids Res 41: 991-995.
4. Berman, H. M., Battistuz, T., Bhat, T. N., Bluhm, W. F., Bourne, P. E., Burkhardt, K., Fagan, (2002) 447 P. The protein data bank. ActaCrystallogr. D. 58, 899-907.
5. C. Belgiovine, E. Bello, M. Liguori, I. Craparotta, L. Mannarino (2017). Lurbinectedin reduces tumour-associated macrophages and the inflammatory tumour microenvironment in preclinical models. Br. J. Cancer, 117 (5) , pp. 628-638.
6. Calimlioglu B, Karagoz K, Sevimoglu T, Kilic E, Gov E and Arga KY (2015). Tissue-Specific Molecular Biomarker Signatures of Type 2 Diabetes: An Integrative Analysis of Transcriptomics and Protein-Protein Interaction Data. OMICS 19: 563-573.
7. Cheng, S., Castillo, V., & Sliva, D. (2019). CDC20 associated with cancer metastasis and novel mushroom-derived CDC20 inhibitors with antimetastatic activity. International Journal of Oncology, 54, 2250-2256. https://doi.org/10.3892/ijo.2019.4791
8. Chin C, Chen S and Wu H (2009). Cyto-Hubba: A Cytoscape Plug-in for Hub Object Analysis in Network Biology. Genome Inform 5: 2-3.
9. Chu, G., Narasimhan, B, Tibshirani, R, Tusher, V.(2001). "SAM "Significance Analysis of Microarrays" Users Guide and technical document."
10. Dallakyan S., Olson A.J. Chemical Biology. Humana Press; New York, NY: (2015). Small-molecule library screening by docking with PyRx; pp. 243–250.
11. D'Amico TA (2008). Molecular biologic staging of lung cancer. Ann Thorac Surg 8 5: S737- S742.
12. DeLano WL (2002) PyMOL. DeLano Scientific, San Carlos, p 700.
13. Dzobo K, Senthebane DA, Rowe A, Thomford NE, Mwapagha LM, Al-Awwad N, Dandara C, Parker MI (2016). Cancer Stem Cell Hypothesis for Therapeutic Innovation in Clinical Oncology? Taking the Root Out, Not Chopping the Leaf. OMICS 20(12): 681-691.
14. Elena Diaz-Rodriguez, " Targeting the Kinetochore in Cancer Therapy: The Ndc80/Hec1 Complex", Current Drug Therapy (2010) 5: 29. https://doi.org/10.2174/1574885511005010029
15. Facchinetti F, Friboulet L. (2019). Profile of entrectinib and its potential in the treatment of ROS1-positive NSCLC: evidence to date. Lung Cancer (Auckl). 10:87-94. doi:10.2147/LCTT.S190786.
16. FDA. FDA approves entrectinib for NTRK solid tumors and ROS-1 NSCLC Available from: https://www.fda.gov/drugs/resources-information-approved-drugs/fda-approves-entrectinib-ntrk-solid-tumors-and-ros-1-nsclc. Accessed August 28, 2019.
17. Gentleman RC, Carey VJ and Bates DM, Bolstad B, Dettling M, Dudoit S, Ellis B, Gautier L, Ge Y, entry J, Hornik K, Hothorn T, Huber W, Iacas S, Irizarry R, Leisch F, Li C, Maechler M, Rossini AJ, Sawitzki G, Smith G, Tierney L, Yang JY, Zhang J (2004). Bioconductor: open software development for computational biology and bioinformatics. Genome Biol 5: R80.
18. Gollapalli K, Ghantasala S, Atak A, Rapole S, Moiyadi A, Epari S, Srivastava S (2017) Tissue Proteome Analysis of Different Grades of Human Gliomas Provides Major Cues for Glioma Pathogenesis. OMICS 21(5): 275-284.

ISSN No. 231-2705 | DOI: 10.51244/IJRSI | Volume X Issue I January 2023

19. Gov E, Kori M, and Arga KY (2017). Multiomics Analysis of Tumor Microenvironment Reveals Gata2 and miRNA-124-3p as Potential Novel Biomarkers in Ovarian Cancer. OMICS 21: 603-615.
20. Gautam, P., Jaiswal, A., Aittokallio, T., Al-Ali, H., & Wennerberg, K. (2019). Phenotypic Screening Combined with Machine Learning for Efficient Identification of Breast Cancer-Selective Therapeutic Targets. *Cell chemical biology*, *26*(7), 970–979.e4. https://doi.org/10.1016/j.chembiol.2019.03.011
21. Gyorffy B, Surowiak P, Budczies J, Lanczky A (2013) . Online survival analysis software to assess the prognostic value of biomarkers using transcriptomic data in non-small-cell lung cancer, PLoS One**,** Dec 18;8(12).
22. Hu M, Qian C, Hu Z, Fei B and Zhou H (2017). Biomarkers in Tumor Microenvironment? Upregulation of Fibroblast Activation Protein-α Correlates with Gastric Cancer Progression and Poor Prognosis. OMICS 21(1): 38-44.
23. Huang, D., Huang, Y., Huang, Z., Weng, J., Zhang, S., & Gu, W. (2019). Relation of *AURKB* over-expression to low survival rate in BCRA and reversine-modulated aurora B kinase in breast cancer cell lines. *Cancer cell international*, *19*, 166. https://doi.org/10.1186/s12935-019-0885-z
24. Irizarry, RA; Hobbs, B; Collin, F; Beazer-Barclay, YD; Antonellis, KJ; Scherf, U; Speed, TP (2003). "Exploration, normalization, and summaries of high density oligonucleotide array probe level data". Biostatistics. 4 (2): 249–64.
25. Janet Piñero, Juan Manuel Ramírez-Anguita, Josep Saüch-Pitarch, Francesco Ronzano, Emilio Centeno, Ferran Sanz, Laura I Furlong, The DisGeNET knowledge platform for disease genomics: 2019 update, *Nucleic Acids Research*, Volume 48, Issue D1, 08 January 2020, Pages D845–D855, https://doi.org/10.1093/nar/gkz1021
26. Jemal A, Siegel R, Ward E, Murray T, Xu J, Thun MJ (2007). Cancer statistics, CA Cancer J Clin 57: 43-66.
27. Karagoz K, Sevimoglu T and Arga KY (2016). Integration of multiple biological features yields high confidence human protein interactome. J Theor Biol 403: 85-96.
28. Kim, S., Chen, J., Cheng, T., Gindulyte, A., He, J., He, S., Zaslavsky, L (2019). PubChem 2019 update: improved access to chemical data. Nuc.Acids Res. 47. D1102-D1109. 530.
29. Komoto, T. T., Bernardes, T. M., Mesquita, T. B., Bortolotto, L., Silva, G., Bitencourt, T. A., Baek, S. J., Marins, M., & Fachin, A. L. (2018). Chalcones Repressed the AURKA and MDR Proteins Involved in Metastasis and Multiple Drug Resistance in Breast Cancer Cell Lines. *Molecules (Basel, Switzerland)*, *23*(8), 2018. https://doi.org/10.3390/molecules23082018
30. Kori M, Gov E and Arga KY (2016). Molecular signatures of ovarian diseases: Insights from network medicine perspective. Syst Biol Reprod Med 62: 266–282.
31. Kuo YH, Lin ZZ, Yang YY, Shao YY, Shau WY, Kuo RN (2012). Survival of patients with small cell lung carcinoma in Taiwan. Oncology; 82:19–24.
32. Kurup A, Hanna NH (2004) Treatment of small cell lung cancer. Crit Rev OncolHematol 52:117–126.
33. Leal J. F., M. Martinez-Diez, V. Garcia-Hernandez, V. Moneo (2010). PM01183, a new DNA minor groove covalent binder with potent in vitro and in vivo anti-tumour activity. Br. J. Pharmacol., 161 (5), pp. 1099-1110.
34. Li X, Zhang L, Yi Z, Zhou J, Song W, Zhao P, Wu J, Song J, Ni Q. NUF2 Is a Potential Immunological and Prognostic Marker for Non-Small-Cell Lung Cancer. J Immunol Res. 2022 May 12;2022:1161931. doi: 10.1155/2022/1161931. PMID: 35600043; PMCID: PMC9119754.
35. Liu, X., Liu, X., Li, J., & Ren, F. (2019). Identification and Integrated Analysis of Key Biomarkers for Diagnosis and Prognosis of Non-Small Cell Lung Cancer. *Medical science monitor : international medical journal of experimental and clinical research*, *25*, 9280–9289. https://doi.org/10.12659
36. Menichincheri M, Ardini E, Magnaghi P (2016). Discovery of entrectinib: a new 3-aminoindazole as a potent anaplastic lymphoma kinase (ALK), c-ros oncogene 1 kinase (ROS1), and pan-tropomyosin receptor kinases (pan-TRKs) inhibitor. J Med Chem; 59(7):3392–3408. doi:10.1021/acs.jmedchem.6b00064.
37. Michael Meister, Anton Belousov, Xu EC, Schnabel P, Warth A, Hoffmann H, Dienemann H, Riedlinger J, Bodenmueller H, Zolg W, Herth FJF, Muley T. Intra-tumor Heterogeneity of Gene Expression Profiles in Early Stage Non-Small Cell Lung Cancer. Journal of Bioinformatics Research Studies 2014, 1(1): 1.
38. Miskolczi Z, Smith MP, Rowling EJ, Ferguson J, Barriuso J, Wellbrock C (2018) Collagen abundance controls phenotypes through lineage-specific microenvironment sensing. Oncogene. doi: 10.1038/s41388018-0209-0.
39. Nie, M., Wang, Y., Yu, Z., Li, X., Deng, Y., Wang, Y., Yang, D., Li, Q., Zeng, X., Ju, J., Liu, M., & Zhao, Q. (2020). AURKB promotes gastric cancer progression via activation of CCND1 expression. Aging, 12(2), 1304–1321. https://doi.org/10.18632/aging.102684
40. Nowak D, Janczak M (2006) Effect of chemotherapy on serum end-products of lipid peroxidation in patients with small cell lung cancer: association with treatment results. Respir Med 100:157–166.
41. Nunez G. Santamaria, C.M. Robles, C. Giraudon, J.F. Martinez-Leal, E. Compe, F. Coin, P. Aviles, C.M. Galmarini, J.M. Egly (2016). Lurbinectedin specifically triggers the degradation of phosphorylated RNA polymerase II and the formation of DNA breaks in cancer cells. Mol. Cancer Ther., 15 (10), pp. 1-14.

ISSN No. 231-2705 | DOI: 10.51244/IJRSI | Volume X Issue I January 2023

42. Ocaña, A., Pérez-Peña, J., Díez-González, L., Sánchez-Corrales, V., Templeton, A., Seruga, B., Amir, E., & Pandiella, A. (2016). Transcriptomic analyses identify association between mitotic kinases, PDZ-binding kinase and BUB1, and clinical outcome in breast cancer. Breast cancer research and treatment, 156(1), 1–8. https://doi.org/10.1007/s10549-016-3720-4
43. Pabla, S., Conroy, J. M., Nesline, M. K., Glenn, S. T., Papanicolau-Sengos, A., Burgher, B., Hagen, J., Giamo, V., Andreas, J., Lenzo, F. L., Yirong, W., Dy, G. K., Yau, E., Early, A., Chen, H., Bshara, W., Madden, K. G., Shirai, K., Dragnev, K., Tafe, L. J., … Morrison, C. (2019). Proliferative potential and resistance to immune checkpoint blockade in lung cancer patients. Journal for immunotherapy of cancer, 7(1), 27. https://doi.org/10.1186/s40425-019-0506-3
44. Pan B, Chen Y, Song H, Xu Y, Wang R, Chen L (2015). Mir-24-3p downregulation contributes to VP16-DDP resistance in small-cell lung cancer by targeting ATG4A. Oncotarget.; 6(1):317-331. doi:10.18632/oncotarget.2787.
45. Patil KR, and Nielsen J (2005). Uncovering transcriptional regulation of metabolism by using metabolic network topology. Proc Natl Acad Sci U S A 102: 2685-2689.
46. Peng Hu, Shangguan J, Zhang L (2015). Downregulation of NUF2 inhibits tumor growth and induces apoptosis by regulating lncRNA AF339813. Int J Clin Exp Pathol. Mar 1;8(3):2638-48.
47. Pettersen, E. F. (2004). UCSF Chimera - A visualization system for exploratory research and analysis. J. Comput. Chem. doi:10.1002/jcc.20084.
48. Qin, S., Long, X., Zhao, Q., & Zhao, W. (2020). Co-Expression Network Analysis Identified Genes Associated with Cancer Stem Cell Characteristics in Lung Squamous Cell Carcinoma. *Cancer investigation*, *38*(1), 13–22. https://doi.org/10.1080/07357907.2019.1697281
49. Salentin S., Schreiber S., Haupt V.J., Adasme M.F., Schroeder M (2015). PLIP: fully automated protein–ligand interaction profiler. Nucleic Acids Res; 43:W443–W447. doi: 10.1093/nar/gkv315.
50. Sevimoglu T, and Arga KY (2014). The role of protein interaction networks in systems biomedicine. Comp Struct Biotech J 11: 22-27.
51. Smyth, G., Yang, Y., and Speed, T. (2003). Statistical issues in cDNA microarray data analysis. Methods in Molecular Biology 224, 111–136.
52. Sun ZY, Wang W, Gao H, Chen QF (2020) . Potential therapeutic targets of the nuclear division cycle 80 (NDC80) complexes genes in lung adenocarcinoma. J Cancer; 11(10):2921-2934. doi:10.7150/jca.41834. Available from https://www.jcancer.org/v11p2921.htm
53. Tang, D., Zhao, X., Zhang, L., Wang, Z., & Wang, C. (2019). Identification of hub genes to regulate breast cancer metastasis to brain by bioinformatics analyses. *Journal of cellular biochemistry*, *120*(6), 9522–9531. https://doi.org/10.1002/jcb.28228
54. Tian Q, Stepaniants SB, Mao M, Weng L, Feetham MC, Doyle MJ, Yi EC, Dai H, Thorsson V, Eng J, Goodlett D, Berger JP, Gunter B, Linseley PS, Stoughton RB, Aebersold R, Collins SJ, Hanlon WA and Hood LE (2004). Integrated genomic and proteomic analyses of gene expression in Mammalian cells. Mol Cell Proteomics 3(10): 960-969.
55. The UniProt Consortium, UniProt: a worldwide hub of protein knowledge, Nucleic Acids Research, Volume 47, Issue D1, 08 January 2019, Pages D506–D515, https://doi.org/10.1093/nar/gky1049.
56. Trigo J., V. Subbiah, B. Besse, V. Moreno (2020). Lurbinectedin as second-line treatment for patients with small-cell lung cancer: a single-arm, open-label, phase 2 basket trial. Lancet Oncol., 21 (5), pp. 645-654.
57. Trott, O., Olson, A.J. (2010). Autodock vina: improving the speed and accuracy of docking with a new scoring function, efficient optimization, and multithreading. Journal of Computational Chemistry 31(2), 455–461.
58. Turanli B and Arga KY (2017). Systems biomedicine acts as a driver for the evolution of pharmacology. Ann Pharmacol Pharm, 2: 1087.
59. Tusher, V. G.; Tibshirani, R (2001). "Significance analysis of microarrays applied to the ionizing radiation response" (PDF). Proceedings of the National Academy of Sciences. **98** (9): 5116-5121.
60. Visualizer, D. S. v4. 0.100. 13345. AccelrysSoftwareInc (2005).
61. VivekSubbiah, Luis Paz-Ares, Benjamin Besse, Victor Moreno (2020). Antitumor activity of lurbinectedin in second-line small cell lung cancer patients who are candidates for re-challenge with the first-line treatment. Lung Cancer, Volume 150, Pages 90-96, ISSN 0169-5002, https://doi.org/10.1016/j.lungcan.2020.10.003.
62. Waterhouse, A., Bertoni, M., Bienert, S., Studer, G., Tauriello, G., Gumienny, R., Heer, F.T., de Beer, T.A.P., Rempfer, C., Bordoli, L., Lepore, R., Schwede, T (2018). SWISS-MODEL: homology modelling of protein structures and complexes. Nucleic Acids Res. 46(W1), W296-W303.
63. Wang, S., Sun, H., Zhan, X., & Wang, Q. (2020). MicroRNA-718 serves a tumor-suppressive role in non-small cell lung cancer by directly targeting CCNB1. International journal of molecular medicine, 45(1), 33–44. https://doi.org/10.3892/ijmm.2019.4396

ISSN No. 231-2705 | DOI: 10.51244/IJRSI | Volume X Issue I January 2023

64. Xiao, Y., Feng, M., Ran, H., Han, X., & Li, X. (2018). Identification of key differentially expressed genes associated with non-small cell lung cancer by bioinformatics analyses. Molecular medicine reports, 17(5), 6379–6386. https://doi.org/10.3892/mmr.2018.8726
65. Xie, B., Wang, S., Jiang, N., & Li, J. J. (2019). Cyclin B1/CDK1-regulated mitochondrial bioenergetics in cell cycle progression and tumor resistance. Cancer letters, 443, 56–66. https://doi.org/10.1016/j.canlet.2018.11.019
66. Xu, S., Liu, R., & Da, Y. (2018). Comparison of tumor related signaling pathways with known compounds to determine potential agents for lung adenocarcinoma. Thoracic cancer, 9(8), 974–988. https://doi.org/10.1111/1759-7714.12773
67. Zhang, Z., Li, M., He, F., Xiang, Z., & Hu, D. (2020). CDK1 serves as a potential prognostic biomarker and target for lung cancer. Journal of International Medical Research. https://doi.org/10.1177/0300060519897508
68. Zhuang, L., Yang, Z., & Meng, Z. (2018). Upregulation of BUB1B, CCNB1, CDC7, CDC20, and MCM3 in Tumor Tissues Predicted Worse Overall Survival and Disease-Free Survival in Hepatocellular Carcinoma Patients. BioMed research international, 2018, 7897346. https://doi.org/10.1155/2018/7897346